EVALUATION OF CANDIDATE THERAPEUTIC AGENTS IN NEURODEGENERATIVE DISEASES

by

Yajas Shah

A thesis submitted to The Johns Hopkins University in conformity with the requirements for the degree of Master of Science

Baltimore, Maryland

August 2017

Abstract

Protein quality control is essential for cellular homeostasis, and defects in the same result in various pathological conditions such as neurodegenerative diseases and cancer. Amyotrophic lateral sclerosis (ALS) is one such condition, involving the degeneration of motor neurons in the central nervous system. Misfolded mutant Superoxide dismutase 1 (SOD1) protein and its aggregates are a hall mark of 15-20% of ALS cases involving hereditary linkage. While several therapeutic strategies, ranging from small molecules to antisense oligonucleotides, have been examined, Riluzole is the only candidate to receive FDA approval for treatment. The purpose of this study is to explore the effect of upregulating p53-mediated transcription as a viable therapeutic strategy. Two compounds were chosen to do so. The study shows that both compounds enhance locomotor activity in $SOD1^{G93A}$ mice, suggesting possible therapeutic applications. Furthermore, one of the compounds reduced the amount of mutant SOD1 aggregates both *in vitro* and *in vivo* suggesting its role in the clearance of misfolded proteins. Although neither of the compounds increased life span, they may be used in conjunction with other molecules, such as Riluzole, to treat ALS.

Thesis Advisor: Dr. Jiou Wang

Thesis Reader: Dr. Philip Jordan

Acknowledgements

Completion of my Master's degree would not have been possible without the hard work, support, encouragement and advice of several people throughout the course of my work both in the Hardwick lab and outside. The time spent working towards achieving this degree has taught me the value of mentorship, guidance, resilience and camaraderie. It has helped me grow both as a person and a scientist.

I would like to start by thanking my thesis and academic advisor Dr. Jiou Wang for his innumerable ideas, support, advice and encouragement throughout this project. I am grateful for his patience and mentorship through these two years. Thank you for giving me a chance to be a part of your wonderful lab and making my experience particularly meaningful.

I would like to thank my thesis reader Dr. Philip Jordan for his knowledgeable inputs and time as well as the provision of animals used in the mass spectrometry experiments. I would also like to thank Dr. Rana Rais and Dr. Sarah Zimmerman for assisting with the mass spectrometry and Dr. J Marie Hardwick for allowing me to use her equipment.

I would like to thank the members of the Wang lab, both past and present for their suggestions, advice, patience and assistance. I would specially like to thank Dr. Tao Zhang, Dr. Yon Ji, Elizabeth Alexander and Justin Chu for their support, mentorship, training and guidance through the project. I would not have been able to complete my work without the

support of everyone else in the Wang Lab. They also created a very enjoyable lab environment in which to work and learn.

Additionally, I would like to thank the BMB department for providing a wonderful work environment as well as invaluable constructive criticism during the departmental retreat.

Above all, I would like to thank my family without which the dream of earning a master's degree would have remained a dream. I greatly appreciate their constant encouragement and moral support.

Lastly, I would like to thank my friends Gibran Nasir, Anton Kvit, Krysynne Leacock, Joshua Hsu, Shengjung Chen, Varsha Srivastan, Adhiraj Yadav and Nukhba Zia for their support and encouragement. I would especially like to thank Prerna Suri for her assistance, ideas, constructive criticism and stimulating conversations through the duration of this project.

Table of Contents

List of Figures

List of Tables

Introduction

Amyotrophic Lateral Sclerosis (ALS; also known as 'Lou Gherig's disease' or 'motor neuron disease') is a progressive degenerative disorder involving atrophy of upper and lower motor neurons in the brain and spinal cord, eventually leading to paralysis followed by death caused by denervation of respiratory muscles, an event that occurs upon five years of diagnosis. Having an annual incidence of 1-2.6 and prevalence of 6 cases per 100,000 individuals respectively coupled with an average age of onset being 58-60 years(Talbott, Malek, & Lacomis, 2016), ALS may be considered the most frequent of the rare neurological diseases. However, its uniform lethality imparts an importance out of proportion with its incidence.

Despite the vast amount of literature available, the exact pathophysiology of ALS remains unknown. Several genetic factors have influenced our understanding of the disease. 10-20% of all ALS cases have been transmitted through families in an autosomal dominant, autosomal recessive or X-linked manner, and is termed as familial ALS (FALS). However, 80-90% of the cases show no distinct genetic linkage and are termed sporadic ALS (SALS)(Corcia et al., 2017).

The first gene implicated in ALS was mapped to the Cu/Zn Superoxide dismutase 1 (SOD1) locus after the assessment of several families. Upon identifying 13 disease causing mutations, they attributed mutant SOD1 to be the cause of 15-20% of all FALS cases, and in turn 1-2% of all ALS cases(Rosen et al., 1993). Ever since, over a hundred disease

causing mutations have been elucidated with the list continuously growing. An updated list for the same may be found at http://alsod.iop.kcl.ac.uk/.

SOD1 is a 153 amino acid cytosolic protein that is ubiquitously expressed in all cell types. It functions as a homodimer which binds two copper and two zinc atoms (one of each per monomer) and partakes in redox chemistry within the cell. It functions to neutralize the superoxide anion (a by-product of oxidative phosphorylation) by converting it to hydrogen peroxide via cyclical oxidation and reduction of copper (dismutation). SOD1 spans across five exons, all of which can contain disease causing missense mutations. While most mutations reduce enzymatic activity, some disease causing (e.g. $SOD1^{G93A}$) ones have no effect on catalysis. This adds to the pre-existing perplexion that none of the mutations are indicative of disease progression and clinical co-relation(Kiernan et al., 2011). However, it has been established that most variants of SOD1 cause ALS in all populations. $SOD1^{A4V}$ has been identified as the most frequent disease causing one in continental United States resulting in it being one of the most studied genotypes. As a result, the current hypotheses suggest a combination of loss-of-function and gain-on-function mechanisms that contribute to the disease.

Post-mortem studies have fueled two primary hypotheses for SOD1-ALS. The initial hypothesis, which fueled the discovery of SOD1-ALS, is that oxidative stress in catalysis deficient motor neurons cause apoptosis. A gain of toxicity mechanism was elucidated on the discovery of SOD1 aggregates when overexpressing wild type SOD1 while co-expressing mutant SOD1 in mice led to disease(Bruijn et al., 1998). Aggregation and/or

deficiencies in protein folding or degradation challenged the pre-existing oxidative stress hypothesis. Several other links suggesting the involvement of aberrant mRNA processing(Yasuda et al., 2017) , glutamate cytotoxicity, altered autophagy and nucleocytoplasmic transport have been proposed. However, while they are noteworthy, they are not directly linked to SOD1-ALS. Admittedly, most cases of ALS have more than one mutated gene, but the scope of this project is to understand the role of SOD1 mutations in isolation.

Transgenic mouse models carrying mutant versions of SOD1 and other ALS genes display cytoplasmic inclusions, mitochondrial dysfunction and motor neuron degeneration similar to that of ALS, and have provided insights to the pathogenesis of the disease, but have failed to predict therapeutic efficacy in humans. Upregulating protein quality control seems to be an ideal strategy for tackling SOD1 inclusions.

Protein quality control refers to the systems cells use to either correctly refold, sequester or degrade abnormal proteins. Under normal conditions, the cells tackle misfolded proteins originating from improper biogenesis, expressed mutant proteins, unassembled subunits of oligomeric proteins and mistranslocated secretory proteins. In addition to these normal sources of misfolded proteins, several pathological conditions such as neurodegenerative diseases and cancer produce a multitude of such variants. While the cell attempts to refold misfolded proteins in most cases, the insurmountable level of proteotoxic stress in SOD1-ALS results in degradation of misfolded proteins.

Targeting protein quality control has been a common strategy to treat ALS. However, several attempts at doing so have failed. Lethal (3) malignant brain tumor like protein 1 (L3MBTL1) and Sirtulin1 (Sirt1) are targets which have not previously been explored for therapeutic potential. Their inhibition serves to increase activity at the p53 promoter, ultimately upregulating protein quality control, a strategy that has recently been explored for its therapeutic potential in models of neurodegenerative disease (Merlo et al., 2014) . This study attempts to understand the effect of inhibiting these genes in murine models of ALS.

Materials and Methods

Cell Based Assays

UNC669 Stock Solution

UNC669 (Abcam) was dissolved in an appropriate amount of DMSO to yield a 200 mM solution. This solution was placed in tinted polypropylene centrifuge tubes and stored at -80 °C for up to two months as per the manufacturer's instructions.

Cell Culture

HEK293T cells (ATCC) were grown in Dulbeccos' Modified Eagle's Medium (DMEM) (Gibco) supplemented with 10% Fetal Bovine Serum (Sigma Aldrich) and 1U Penicillin/1 µg Streptomycin (Invitrogen). Cells were incubated at 37 °C and 5% CO2 in a humidified chamber.

Transfection

HEK293T cells were seeded in six 60 mm culture dishes at a density of 400,000 cells per dish. After 24 hours, cells from five out of six dishes were transfected with 150 ng of BOS-SOD1G85R plasmid using 3 µl of JetPRIME reagent (Polyplus) and 200 µl of JetPRIME buffer (Polyplus) as per the manufacturer's instructions.

UNC669 Treatment and Cell Harvest

24 hours post transfection, the culture media was aspirated and replaced with 4 mL of DMEM. UNC669 dissolved in DMSO was added to the transfected wells with a total concentration of 0 µM, 25 µM, 50 µM, 100 µM and 200 µM in each dish respectively.

Following 24 hours of treatment, the media was aspirated and replaced by 220 µL of a lysis buffer containing 5% IGEPAL-630, 1x Protease Inhibitor Cocktail (Sigma Aldrich) and 0.25 mM Iodoacetamide (Sigma Aldrich). Cells were incubated on ice with the lysis buffer for three minutes, following which they were scraped off the wells. The lysates obtained were individually collected in polypropylene centrifuge tubes and sonicated for two intervals of five minutes each at 4°C on high settings (30 seconds on, 30 seconds off). Sonicated lysates were stored at -80 °C until further use.

Fractionation

Sonicated lysates were thawed on ice and transferred to air-driven ultracentrifuge tubes (Beckman Coulter). The lysates were centrifuged at ambient temperature using an Airfuge Air-Driven Ultracentrifuge (10 minutes, 25,000 psi) (Beckman Coulter). The supernatant was collected in fresh centrifuge tubes and labelled as S1 fractions. The pellet was washed using a buffer containing 5 M IGEPAL-630, and resuspended in 110 µL of a buffer containing 5% SDS, 8 M Urea, 0.1 mM EDTA and 40 mM Tris-Cl ph 6.8. Resuspended pellets were sonicated at 15-20 °C for six intervals of five minutes each on high settings (30 seconds on, 30 seconds off). Upon sonication, the lysates were labelled as the P2 fractions. Lysates were stored at -80 °C until further use. Protein concentration in the lysates was determined by the BCA assay (Thermo Fisher).

Western Blot

S1 and P2 samples were aliquoted in 6x SDS sample loading buffer containing 0.375M Tris pH 6.8, 12% SDS, 60% glycerol, 0.6M DTT and 0.06% bromophenol blue to obtain

15 µg of protein per sample. Samples were placed in a heating block at 95 °C for five minutes, following which they were centrifuged at ambient temperature for three minutes at 12,000 rpm. Protein lysates were resolved by SDS-PAGE on 4-20% Criterion TGX precast SDS gels (BioRad) at 100V. Upon resolution, proteins were transferred to nitrocellulose membranes using the semi-dry Transblot system (BioRad). Membranes were incubated in blocking buffer containing 5% non-fat dry milk (Sigma Aldrich) in TBS-T (20 mM Tris, 150 mM NaCl, pH7.6, 0.1% Tween®20) on a shaker for two hours. Membranes were washed thrice x five min each with TBS-T following overnight incubation with primary antibodies [1:3000 polyclonal SOD rabbit (Enzo Life Sciences) and 1:2000 ß-Actin clone 4, mouse (SantaCruz Biotech)] in TBS-T containing 5% Bovine Serum Albumin (Sigma Aldrich). The membranes were washed thrice x 5 min each with 5% TBS-T, and incubated with secondary antibody [1:10000 IRDye Anti-mouse IgG linked with 680RD (Licor) and 1:1000 IRDye Anti-rabbit IgG linked with 800LT (Licor)] on a shaker at room temperature for one hour. The membrane was washed thrice x 5 minutes each with TBS-T, and imaged on a Licor Odessey imager at 700 nm and 800 nm and quantified using ImageStudio.

Animal Based Assays

Animal Housing and Selection of Experimental Animals

B6.Cg-Tg(SOD1*G93A)1Gur/J males as well as C57BL/6J females were obtained from the Jackson Laboratory. Breeding cages were set up with one male and two females. Animals were housed in the institutional animal facility (12 hours white light, 12 hours red light) at 72 °C, 48% relative humidity and fed regular chow and water *ad libitum* as

approved by the institutional animal care and use committee (IACUC). Mice were genotyped using PCR, followed by qPCR for analysis of *SOD1*^{G93A} copy number variations. Only gender matched littermates which had a high copy number (>23) were selected for experimentation. For PCR genotyping, oIMR0113 (CAT CAG CCC TAA TCC ATC TGA) and oIMR0114 (CGC GAC TAA CAA TCA AAG TGA) were used to amplify the *SOD1*^{G93A} transgene, while oIMR7338 (CTA GGC CAC AGA ATT GAA AGA TCT) and oIMR7339 (GTA GGT GGA AAT TCT AGC ATC ATC C) served as internal positive controls. Upon amplification, the products were electrophoresed on a 1.5% agarose gel at 90V and subsequently imaged on a UV transilluminator. For copy number analysis, oIMR1544 (CAC GTG GGC TCC AGC ATT) and oIMR3580 (TCA CCA GTC ATT TCT GCC TTT G) served as internal positive controls while oIMR9665 (GGG AAG CTG TTG TCC CAA G) and oIMR9666 (CAA GGG GAG GTA AAA GAG AGC) were used to amplify *SOD1*^{G93A}. All reactions were performed as per the instructions provided by the Jackson Laboratory.

Euthanasia

The humane end point of the experiment was when a mouse could not right itself after being placed on its back for 30 seconds. At this point, mice were euthanized in an enclosed chamber injected with CO2 at a flow rate of 10 psi for ten minutes in accordance with the IACUC guidelines.

Intraperitoneal Injections

UNC669 (Abcam) was dissolved in an appropriate amount of DMSO and diluted with Dulbecco's Phosphate Buffered Saline (DPBS) (Gibco) to yield a 10 mM and 30 mM solution containing 10% DMSO (v/v). The solution was aliquoted in tinted vials at -20 °C for up to two months. Tenovin-6 (Adooq Biosciences) was dissolved in an appropriate amount of DMSO and diluted with Dulbecco's Phosphate Buffered Saline (DPBS) (Gibco) to yield a 4.5 mM solution containing 10% DMSO (v/v). The solution was aliquoted in tinted vials at -20 °C for up to two months. A blank vehicle mix was prepared and stored at 4 °C for up to two months. Gender and litter-matched transgenic pairs of mice aged 35 days were injected with either UNC669 (10 mM or 30 mM), Tenovin-6 4.5 mM or vehicle (10% DMSO dissolved in DPBS (Gibco)) intra-peritoneally (I.P.) at 5 mL/kg mouse. The injections were subsequently repeated every five days.

Rotarod Assay

Experimental mice were trained on the Rotarod apparatus (4-32 rpm over 5 minutes) (Harvard Apparatus) at the age of 36 days, and subsequently every week. Mice were given three attempts, after which they were returned to their cages. Experimental mice were tested a day after training. The time taken for mice to fall off the rotarod was noted. Data was collected for 16 weeks in triplicates and mice were given 1 minute to recover before each trial. The assay was performed on a weekly basis. Both training and testing were performed at a fixed time to prevent confounding factors such as the circadian rhythm.

Body Weight

Body weight measurements were taken on a weekly basis prior to conducting the rotarod assay.

Grip Strength Assay

The strength of all four limbs in combination of experimental mice was assayed using the grip strength apparatus (Bioseb) in triplicates. Mice were placed on a perforated grill and pulled off it at an angle parallel to the workspace. Data was collected on the highest setting, and any force greater than 25 N was recorded. The assay was performed at a fixed time to prevent confounding.

Survival Analyses

Experimental animals were monitored daily for survival analysis. The humane end point was considered the point at which the mouse cannot right itself within 30 seconds of being placed on its side, and the age of the mouse was recorded when it reached this phenotype following euthanasia as per IACUC guidelines.

Tissue Harvest, Lysate Preparation and Western Blot

Experimental mice were euthanized at the age of 150 days using a CO_2 chamber as per IACUC guidelines. The mice were dissected, and organs were harvested in polypropylene centrifuge tubes followed by snap freezing them in liquid nitrogen. All harvested organs were stored at -80 °C until further use. Organs were weighed and submerged in two times

the volume of a lysis buffer containing 5% IGEPAL-630, 1x Protease Inhibitor Cocktail (Sigma Aldrich), and 0.25 mM Iodoacetamide (Sigma Aldrich) on ice. Subsequent steps of lysate preparation, fractionation and western blotting were carried out with the same method used for cell culture.

Mass Spectrometry

Preparation of standard and internal standard (IS) stock solution

UNC669 was dissolved in an appropriate amount of DMSO to yield a 10 mM stock solution, which was stored in tinted tubes at -20°C. Similarly, Tenovin-6 was dissolved in DMSO to yield a 10 mM stock solution and subsequently stored at -20°C. Losartan (IS) was dissolved in DMSO to obtain a 10 mM stock solution. This was subsequently diluted to obtain a 500 nM solution which was stored at -20°C.

Standard Curve and Quality Control (QC) Sample Preparation

Standard curve plasma samples were prepared using naïve mouse plasma or naïve mouse brain homogenates. Standard curves for both these fractions were prepared by serially diluting the stock solution, with 7 standards and 3 QCs ranging from 10 to 10,000 nM in mouse plasma and in mouse brain homogenate matrix for UNC669 and 7 standards and 4 QCs ranging from 50 to 50,000 nM in mouse plasma and 6 standards and 2 QCs from 5 to 1,000 nM in mouse brain homogenate matrix.

Extraction Procedure

Plasma: UNC669 was extracted from plasma samples by precipitating proteins using acetonitrile. Briefly standards, QCs, and samples (50 µL) were mixed with 300 µL acetonitrile containing 0.5 µL Losartan (IS) in low retention microcentrifuge tubes. The mixtures were vortexed for 1 min and subsequently centrifuged at 10,000 rpm for 10 min at 4°C (Eppendorf 5417R). 50 µL of the supernatant was transferred to a 250 µL polypropylene autosampler vial and mixed with 50 µL of water, and sealed with a Teflon cap. A volume of 3 µL was injected onto the ultra high performance liquid chromatography (UHPLC) instrument (Accela pump 1250 and Accela autosampler AS, Thermo Scientific) for quantitative analysis using a temperature controlled autosampler operating at 10°C.

Tenovin-6 was extracted from plasma samples by protein precipitation using acetonitrile. Briefly standards, QCs, and samples (25 µL) were mixed with 125 µL acetonitrile containing 0.5 µM Losartan (internal standard; IS) in low retention microcentrifuge tubes. The mixture was vortexed for 1 min and centrifuged at 10,000 rpm for 10 min at 4°C. 50 µL of supernatant was transferred to a 250 µL polypropylene autosampler vials and mixed with 50 µL water, and sealed with a Teflon cap. A volume of 3 µL was injected onto the ultra-performance liquid chromatography (UPLC) instrument for quantitative analysis using a temperature-controlled autosampler operating at 10 °C.

Brain and Spinal Cord: For analysis of tissue samples, standard curve and quality control samples were prepared using the brain matrix. For extraction of UNC669, brain and spinal cord samples were weighed and extracted with two times the volume of acetonitrile. Samples were subsequently placed in -20°C for 30 min and pulverized, followed by vortexing and centrifugation 10,000 rpm at 4°C for 10 min. 50 µL of the supernatant was

transferred to a 250 µL polypropylene autosampler vial and was mixed with water containing 20 µM Losartan, and sealed with a Teflon cap. A volume of 3 µL was injected onto the ultra high performance liquid chromatography (UHPLC) instrument (Accela pump 1250 and Accela autosampler AS, Thermo Scientific) for quantitative analysis using a temperature controlled autosampler operating at 10°C.

For analysis of tissue samples, standard curve and quality control samples were prepared using brain matrix. For extraction of Tenovin-6, spinal cord and brain samples were weighed, and extracted with two times the volume of acetonitrile. Samples were placed in -20°C for 30 min and pulverized, followed by vortexing and centrifugation 10,000 rpm at 4°C for 10 minutes. 50 µL of supernatant was transferred to a 250 µL polypropylene autosampler vials and was mixed with 50 µL water with 0.05 µM Losartan, and sealed with a Teflon cap. A volume of 3 µL was injected onto the ultra-performance liquid chromatography (UPLC) instrument for quantitative analysis using a temperature-controlled autosampler operating at 10°C.

Chromatographic and Mass Spectrometric Conditions

UNC669:

UHPLC System: Accela pump 1250 and Accela open-arm autosampler AS

Column: Eclipse Plus C18 RRHD 1.8 µm, 2.1 x 100 mm

Flow Rate: 0.4 mL/min

Mobile Phase A: 0.1% FA in CAN

Phase B: 0.1% FA in water

LC Gradient Condition:

Time (min)	Phase A (%)	Phase B (%)
0.01	10	90
0.20	10	90
2.00	99	1
2.50	99	1
2.70	10	90
4.50	10	90

Table 1: Liquid chromatography gradient conditions for UNC669

Tenovin-6:

UHPLC System: Accela pump 1250 and Accela open-arm autosampler AS

Columns: Xterra MS C18 3.5 µm, 2.1x50 mm

Flow rate: 0.4 mL/min

Mobile Phase A: 0.1% FA in ACN,

Phase B: 0.1% FA in water.

LC Gradient Condition:

Time (min)	Phase A (%)	Phase B (%)
0.01	5	95
0.20	5	95
2.00	99	1
2.50	99	1

2.70	5	95
4.50	5	95

Table 2: Liquid chromatography gradient conditions for Tenovin-6

Mass Spectrometry Conditions

MS: TSQ Vantage (Thermo Scientific)

UNC669 Conditions:

Ionization Mode	ESI, MRM (+)			
Compound	Q1	Q3	CE	S-Lens
UNC669	337.887	155.913, 183.920	47, 30	96
Losartan	423.200	180.088, 207.107	35, 22	99

Table 3: Mass spectrometry conditions for UNC669

The mass spectrometer was operated with an ESI interface with positive ionization mode for UNC669 and controlled by the Xcalibur software 2.3 (Thermo Scientific). Samples were introduced to the interface through Turbo Ion Spray with the capillary temperature setting at 350°C. Nitrogen was used as the sheath and auxiliary gas with settings of 40 and 5, respectively. Quantification was performed in multiple reaction monitoring (MRM) mode.

Tenovin-6 Conditions

Ionization Mode	ESI, MRM (+)			
Compound	Q1	Q3	CE	S-Lens
Tenovin-6	494.975	233.027, 278.115	30, 19	102
Losartan	422.860	180.090, 207.113	32, 18	89

Table 4: Mass spectrometry conditions for Tenovin-6

The mass spectrometer was operated with an ESI interface in positive ionization mode for Tenovin-6 and controlled by the Xcalibur software 2.3 (Thermo Scientific). Samples were introduced to the interface through Turbo Ion Spray with the capillary temperature setting at 350°C. Nitrogen was used as the sheath and auxiliary gas with the settings of 40 and 5, respectively. Quantification was performed in multiple-reaction monitoring (MRM) mode. Chromatographic analysis was performed using an AccelaTM ultra high-performance system consisting of an analytical pump, and an autosampler coupled with TSQ Vantage mass spectrometer (Thermo Fisher Scientific Inc., Waltham MA). Separation of the analyte from plasma, brain and spinal cord matrices was achieved at ambient temperature using a Waters Xterra MS C18 (2.1 x 50 mm) packed with a 3.5 µm C18 stationary phase. The mobile phase used was composed of 0.1% Formic Acid in Acetonitrile and 0.1% Formic Acid in water with gradient elution, starting with 5 % organic linearly increasing to 99% at 2 min, maintaining at 99% (2-2.5 min), re-equilibrating to 5 % by 2.7 min and

maintaining 5 % organic until the end of the run. The total run time for each analyte was 4.50 min.

Data were acquired by Xcalibur software. Chromatographic peaks for analyte transitions were integrated and quantified to calculate the concentration of each peak based on the calibration curve. Calibration curves for Tenovin-6 were computed using the ratio of the peak area of analyte to the internal standard by using a quadratic regression with 1/x weighting. The parameters of each calibration curve were used to back-calculate concentrations and to obtain values for the QC samples and unknown samples by interpolation.

Results

UNC669 shows rapid penetration and clearance from tissues

Several compounds have been assessed for their efficacy to treat ALS(Jiang et al., 2014; Mancuso et al., 2012; Mancuso et al., 2014; Traynor et al., 2006). However, only Riluzole has been approved by the FDA for treatment(Bruijn, Miller, & Cleveland, 2004; Lacomblez, 1996) . Although these compounds may be delivered in several ways, their distribution across the central nervous system is of immense importance(Bryson & Bryson, 1996; Prathyusha Vikram, 2017) . UNC669 has been recently characterized an L3MBTL1 inhibitor(Herold et al., 2012; Zhou et al., 2016) and has not been used in animal models for therapeutic applications. To assess the optimum dosage, we injected mice with a standard pharmacokinetic dose (10 mg/kg and 5 mL/kg, which equated to 100 μL of a 10 mM solution delivered to a 20g mouse) and analyzed its distribution in the plasma, brain and spinal cord using mass spectrometry over a time course of three hours.

Mice administered UNC669 intraperitoneally accumulate the compound in the plasma, brain and spinal cord within 30 minutes but is significantly cleared in 3 hours (Fig. 1C). At 30 minutes, the plasma contains 2724 pmol/mL of UNC669. However, the brain and spinal cord contains 5308 pmol/g and 3763 pmol/g respectively at the same time point, suggesting that UNC669 readily crosses the blood-brain barrier. Greater accumulation of UNC669 in the brain and spinal cord than plasma at the 3 hour time point reinforce greater distribution of the compound across the blood-brain barrier. While it readily crosses the blood-brain barrier, all tissues significantly cleared most of UNC669 after three hours of administration. Although the dosage was optimized, the dose which causes a physiological

response could not be identified by this experiment. As a result, two doses (10 mM and 30 mM) were selected for further experimentation.

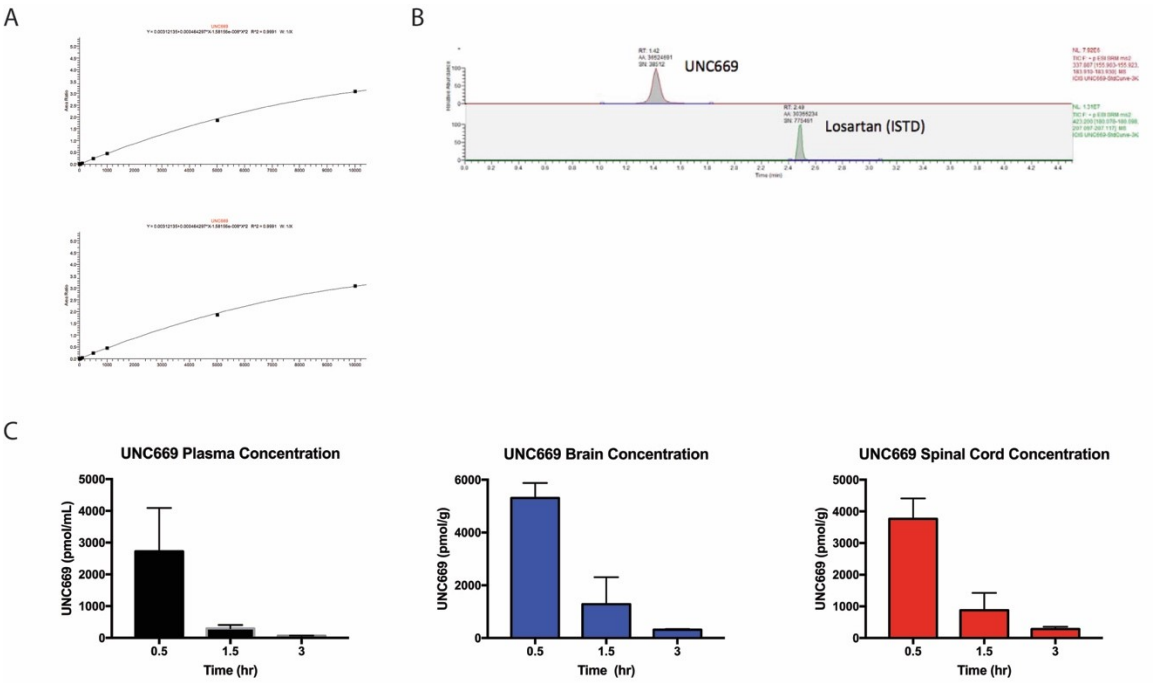

Fig. 1: (A) Standard curves for UNC669 in plasma (above) and brain (below) with (B) a representative chromatogram peak for UNC669. Losartan served as an internal control. (C) Concentration of UNC669 in plasma (left), brain (middle) and spinal cord (right) over a time course of three hours post IP injection

Trends in body weight progression in UNC669 trials

Body weight is an essential parameter in understanding degeneration through behavioral experiments. The onset of ALS involves rapid degeneration of motor neurons, which results in non-recoverable weight loss. Our C57BL/6J mice containing the SOD1^{G93A} transgene that go on to develop ALS also show such patterns.

Both the treated and untreated groups of mice begin to show a loss in weight at an age of 19 weeks in the UNC669 10 mM trial (Fig. 2A). Although the vehicle injected mice appear to weigh slightly more than UNC669 10 mM treated mice, the difference is not significant. The same trend was observed in both groups (Fig. 2A).

Concurrent with the findings above, the UNC669 30 mM trial showed similar trends with the average age of non-recoverable weight loss at 18 weeks (Fig. 3A). Furthermore, there was no difference in body weight between the two groups (Fig. 3A).

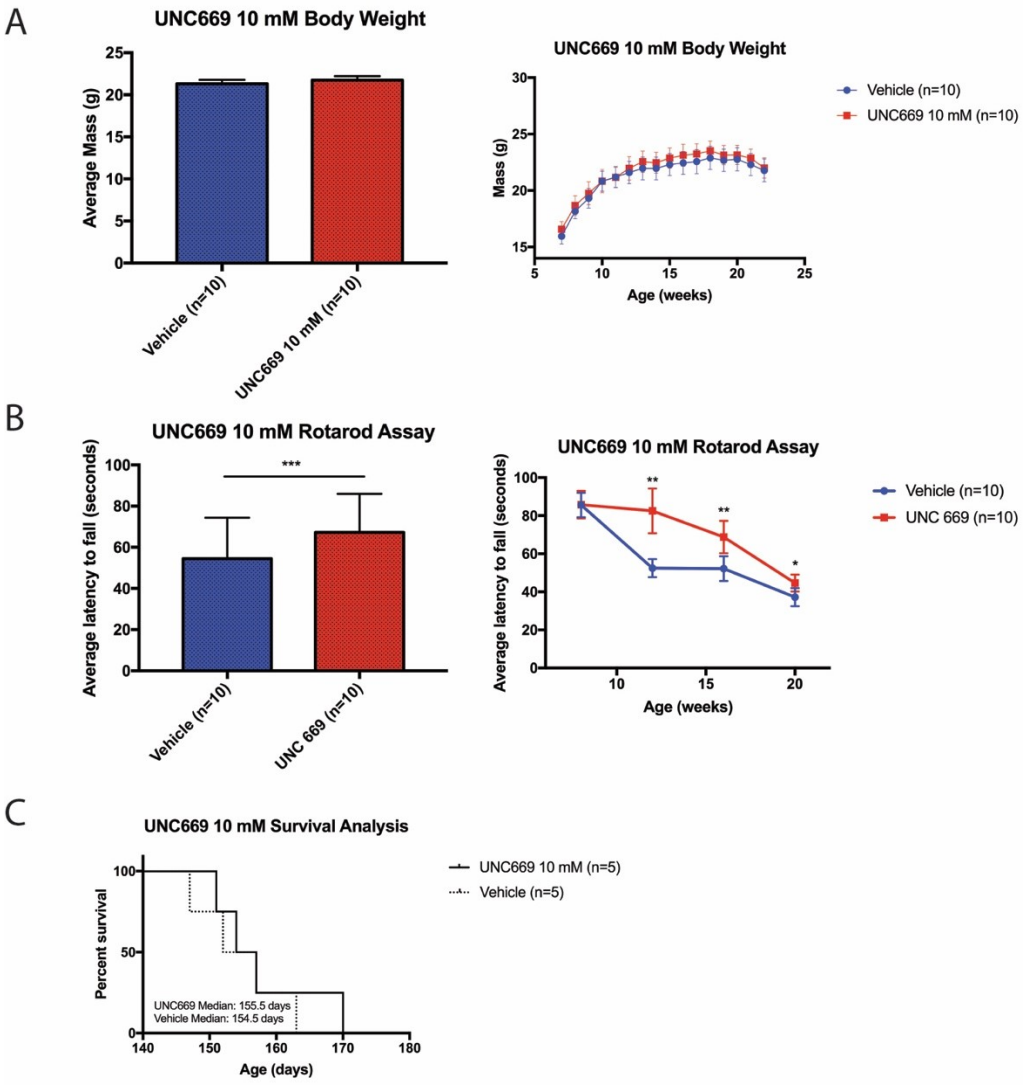

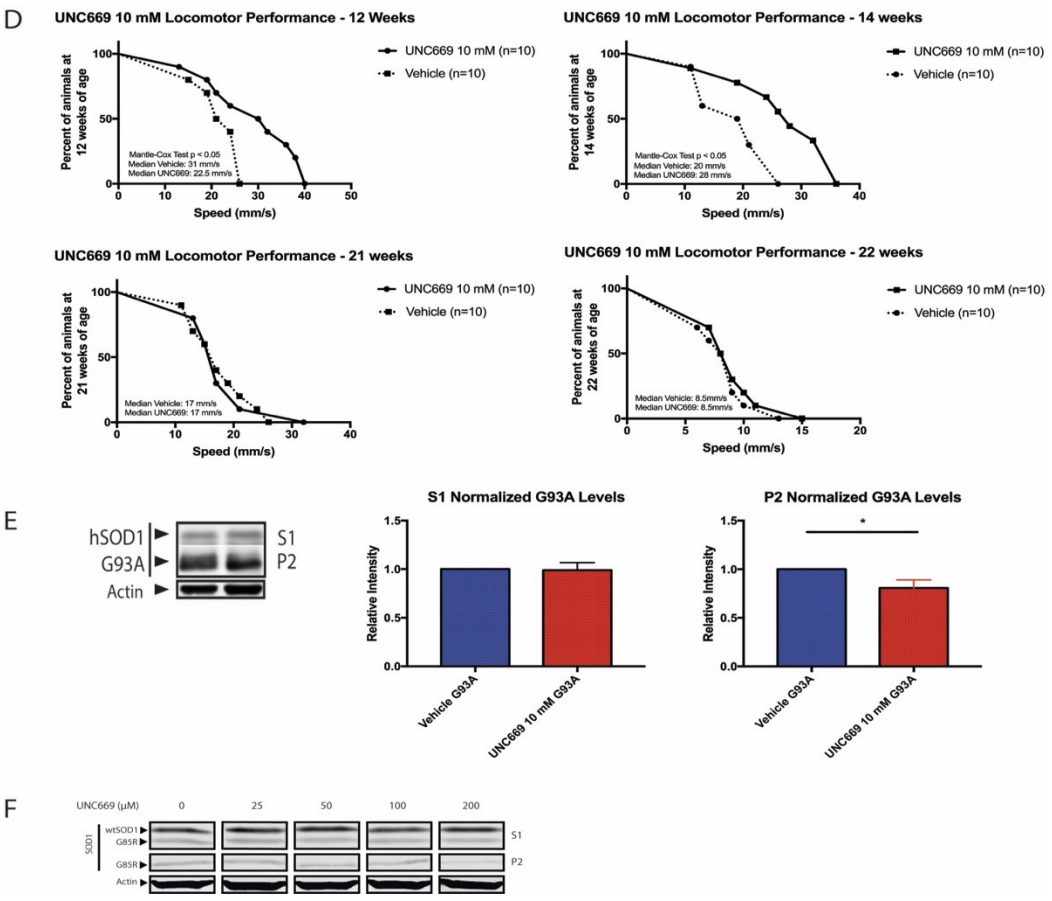

Fig. 2: SOD1^{G93A} mice treated with 10 mM UNC669 showed (A) similar trends in body weight but (B) exhibited a greater latency to fall off the rotarod as compared to the vehicle treated group. (C) UNC669 treatment did not have an effect on the life span. (D) The median maximum speed attained by UNC669 treated mice was significantly greater than the vehicle group at ages of 12 and 14 weeks, while there was no difference between the groups at ages of 20 and 21 weeks. (E) Western blots of UNC669 10 mM trial brain tissue show significantly less SOD1^{G93A} in the P2 fraction. A similar trend was observed in (F) HEK293T cells transfected with SOD1^{G85R} and treated with UNC669.

UNC669 does not improve grip strength

Neuromuscular strength has been shown to decrease with disease onset due to degeneration of motor neurons(Knippenberg, Thau, Dengler, & Petri, 2010; Smittkamp, Brown, & Stanford, 2008; Wilson, Petrik, Moghadasian, & Shaw, 2005) . To see if there was a difference in muscular strength in mice that have been treated with UNC669 vs their untreated counterparts, forelimb strength was chosen as a parameter. There was no observable difference between the test and treated groups of mice (data not shown). However, at the age of 12 weeks there seemed to be an increased difference between the test and treated groups, with vehicle showing slightly increased forelimb strength (data not shown). When mice were dosed with 30 mM of UNC669, there was no observable difference between the test and treated mice through the course of the experiment (Fig. 3B).

UNC669 improves locomotor ability in mice subjected to a 10 mM solution

Muscular activity is an essential parameter for assessing paralysis caused by ALS. While mild paralysis begins slightly before the onset of disease, muscular activity of hind limbs exponentially decreases as the disease progresses(Knippenberg et al., 2010; Wilson et al., 2005) . To test for change in muscular activity, mice were placed on a rotarod, which is an accelerating rod that enables assessment of reduced locomotive abilities. As locomotor activity reduces, mice lose the ability to stay on the rod for longer periods of time. Hence, shorter time on the rotarod hints at reduced muscular activity and hence possible increased progression of disease.

Mice administered a 10 mM solution of UNC669 performed significantly better in the rotarod assay than the control (Fig. 2C). Treated mice were able to stay on the rod for a longer period of time than the untreated group from 11 weeks of age up to the point they met the euthanasia criteria. It was noted that the difference in locomotor ability, which can be read as a latency to fall off the rod, between the treated and untreated mice varied with time. The biggest difference between the groups was observed at an age of 12 weeks. However, the difference in latency to fall diminished with an increase in time, suggesting an age-dependent response to the drug. A possible reason for the age-dependent response is a threshold for UNC669 mediated protein quality control, beyond which the misfolding stress is too high. In contrast, mice treated with a 30 mM solution of UNC669 did not perform better than the vehicle at any point (Fig. 3C).

UNC669 10 mM treatment did not increase the life span of mice

Survival curves are essential to determine if a test compound has the therapeutic effect to increase lifespan. The behavioral end point used was the day at which a mouse cannot right itself after 30 seconds of turning it on its back, as used in several other studies. While it is well recognized that female $SOD1^{G93A}$ mice live up to a week longer than their male counterparts, both males and females were used in the study and they were not analyzed separately.

The UNC669 10 mM treated group median life span was one day greater than that of the vehicle, but the difference was not statistically significant (Fig. 2D). Similarly, the UNC669 30 mM treated group reached the end point at the same it its control group did (Fig. 3D).

UNC669 10 mM treated mice run faster than vehicle treated mice

Locomotor activity can also be studied by the speed at which mice can travel on the rotarod. The speed (in rpm) at which mice fell off the rotarod was noted, and converted to mm/s using the formula $v = r \times \omega \times 1000$. The median values were compared between treated and untreated groups at several time points.

The median speed at which mice fell off the rotarod was found to be significantly higher in the UNC669 treated group than the vehicle at 12 weeks and 14 weeks of age (Fig. 2E). However, there was no difference between the two groups at the end of the trial at 20 weeks and 21 weeks respectively (Fig. 2E).

UNC669 treatment did no alter the age of onset

Disease onset was analyzed by observing gait, ability to walk and the righting reflex while scoring it from 1-5 on a modified Neurological Scoring System(Hatzipetros et al., 2015) . A score of 1 suggests that the mouse is pre-symptomatic while a score of 5 suggests that the mouse has reached its humane end point.

The median amount of time for mice to reach stage 5 was found to be identical for both 10 mM and 30 mM UNC669 treatment groups as well as their controls (data not shown). However, it was noticed on random occasion that some mice meet the euthanasia requirements only a day after reaching stage 5, while others could endure for over a week. No trends were observed between pairs, and this seemed to be unpredictable.

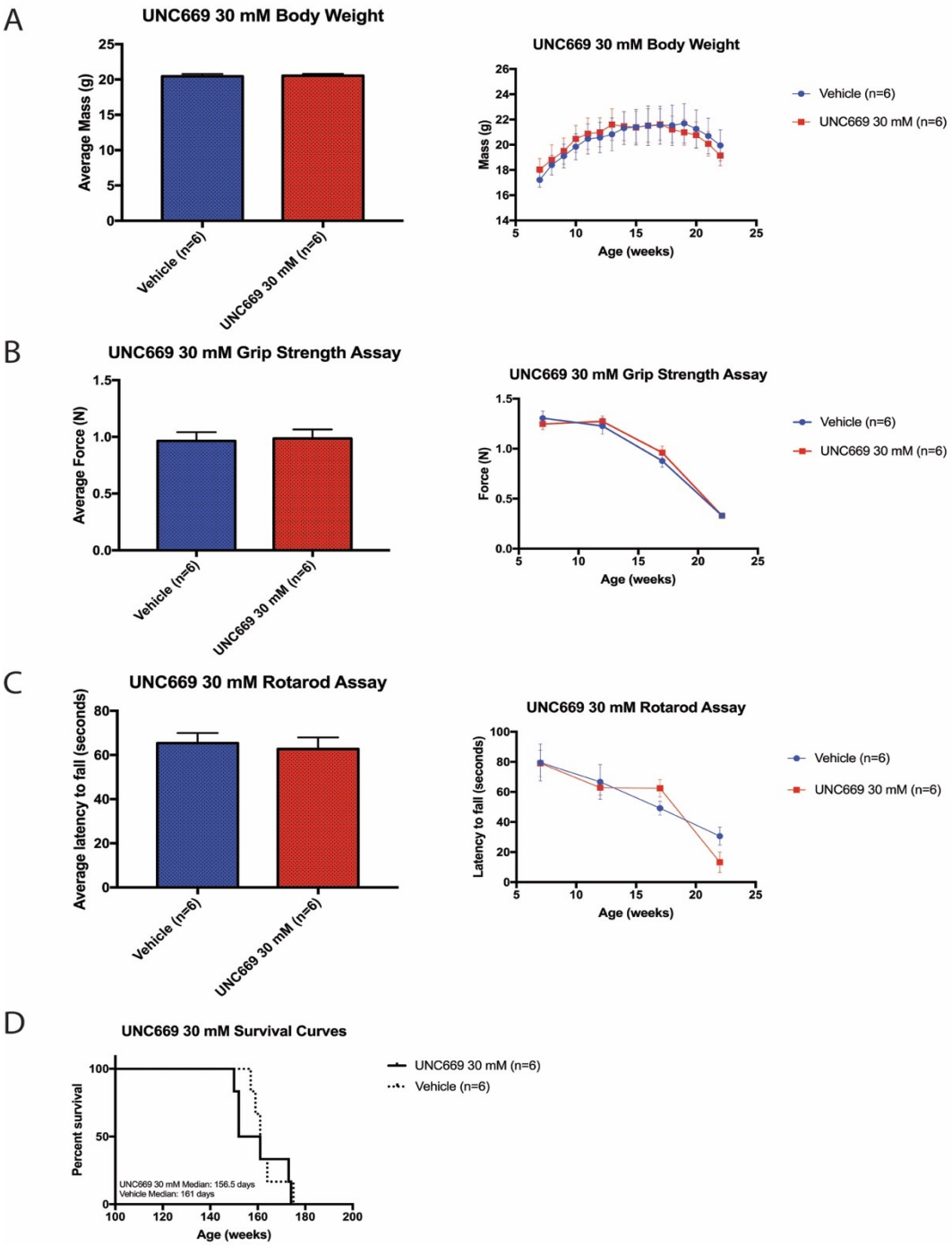

Fig. 3: Mice treated with UNC669 30 mM show no significant differences from vehicle groups in (A) body weight, (B) grip strength, (C) locomotor activity or (D) life span.

UNC669 reduces the amount of aggregates *in vitro* and *in vivo*

Evidence highlights a toxic gain-of-function mechanism of disease for mutant SOD1 linked ALS(Bruijn et al., 2004; Kiernan et al., 2011) . SOD1 aggregates serve to be the pathogenic determinant for disease(Bruijn et al., 1998; Kiernan et al., 2011; Watanabe et al., 2001) . The G93A mutation does not compromise the enzymatic activity of SOD1 even in aggregates(Scott et al., 2008). While SOD1 knockout models obviously show aspects of disease, some of which are related to motor neurons, but conclusive evidence linking SOD1 loss-of-function to ALS does not exist(Rachele A Saccon, Rosie K A Bunton-Stasyshyn, Elizabeth M C Fisher, & Pietro Fratta, 2013) .

To understand the effects of UNC669 on SOD1 aggregates, we used an assay to separate small aggregates (S1 fraction) from large aggregates (P2 fractions) based on their solubility.

A dose-dependent response was observed on transfecting HEK293T cells with *SOD1*^{G85R} and treating them with UNC669. While the fraction containing soluble aggregates remained unchanged over all concentrations, there was a reduction in larger insoluble aggregates at concentrations of 50 µM, 100 µM and 200 µM (Fig. 2G). A similar trend was observed in brains isolated from of UNC669 10 mM treated mice, where the amount of large aggregates were 20% less than that of the control (Fig. 2F). The reduction in the amount of large aggregates, a highly toxic species, coupled with no effect in soluble SOD1$^{G85R/G93A}$ suggests that this may be a mechanism for cells to counteract protein misfolding stress. Constant levels of the less toxic soluble species could purport the argument that UCN669 exerts its effects in transcription-independent mechanisms.

Tenovin-6 shows slower penetration into tissues coupled with saturation kinetics

Mice administered Tenovin-6 intraperitoneally at a concentration of 10 mg/kg and 5 mL/kg of the mouse saturate the brain and spinal cord. While the concentration of Tenovin-6 in plasma decreases over 3 hours, the brain and spinal cord levels remain constant (Fig. 4C). Interestingly, the spinal cord significantly accumulates less Tenovin-6 at the 1.5 hour time point as compared to 0.5 hours and 3 hours, a trend that is not present in the brain. Furthermore, spinal cord accumulation is driven in part by direct transmission of cerebrospinal fluid (CSF) from the brain. While this experiment cannot determine causation for this phenomenon, it is possible that fraction of Tenovin-6 in the brain may be largely concentrated in cells which suggest that CSF may be saturated at extremely low levels of Tenovin-6. This hypothesis coupled with a faster turnover in the spinal cord than the brain may explain the reduction of Tenovin-6 concentration at the 1.5 hour time point.

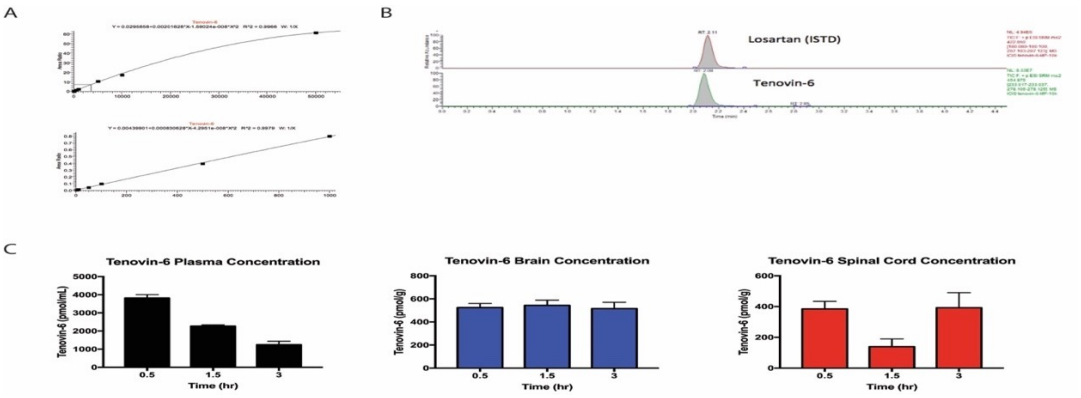

Fig. 4: (A) Standard curves for Tenovin-6 in plasma (above) and brain (below tissue) with (B) a representative chromatogram peak for Tenovin-6. Losartan served as an internal control. (C) Concentration of Tenovin-6 over in plasma (left), brain (middle) and spinal cord (right) in a time course of three hours post IP injection

Tenovin-6 4.5 mM treated mice weighed less than the vehicle

While both groups of mice showed similar trends in weight gain and loss, the vehicle group had a greater mean body weight than the Tenovin-6 group (Fig. 5A). However, the treated group had a greater mean body weight at the end of the trial than the vehicle group.

Tenovin-6 4.5 mM treated mice did not exhibit increased grip strength ability

Although the Tenovin-6 4.5 mM group showed slightly improved grip strength in the middle of the trial, the effect wore of as the trial progressed (Fig. 5B). Furthermore, the mean grip strength for both groups was almost identical. Similar trends were observed in both groups and no difference between the groups was noted.

Tenovin-6 4.5 mM treated mice show better locomotor activity

Tenovin-6 4.5 mM treaded mice have a greater average latency to fall of the rotarod when all time points are considered(Fig. 5C). However, this difference is not significant towards the end of the trial.

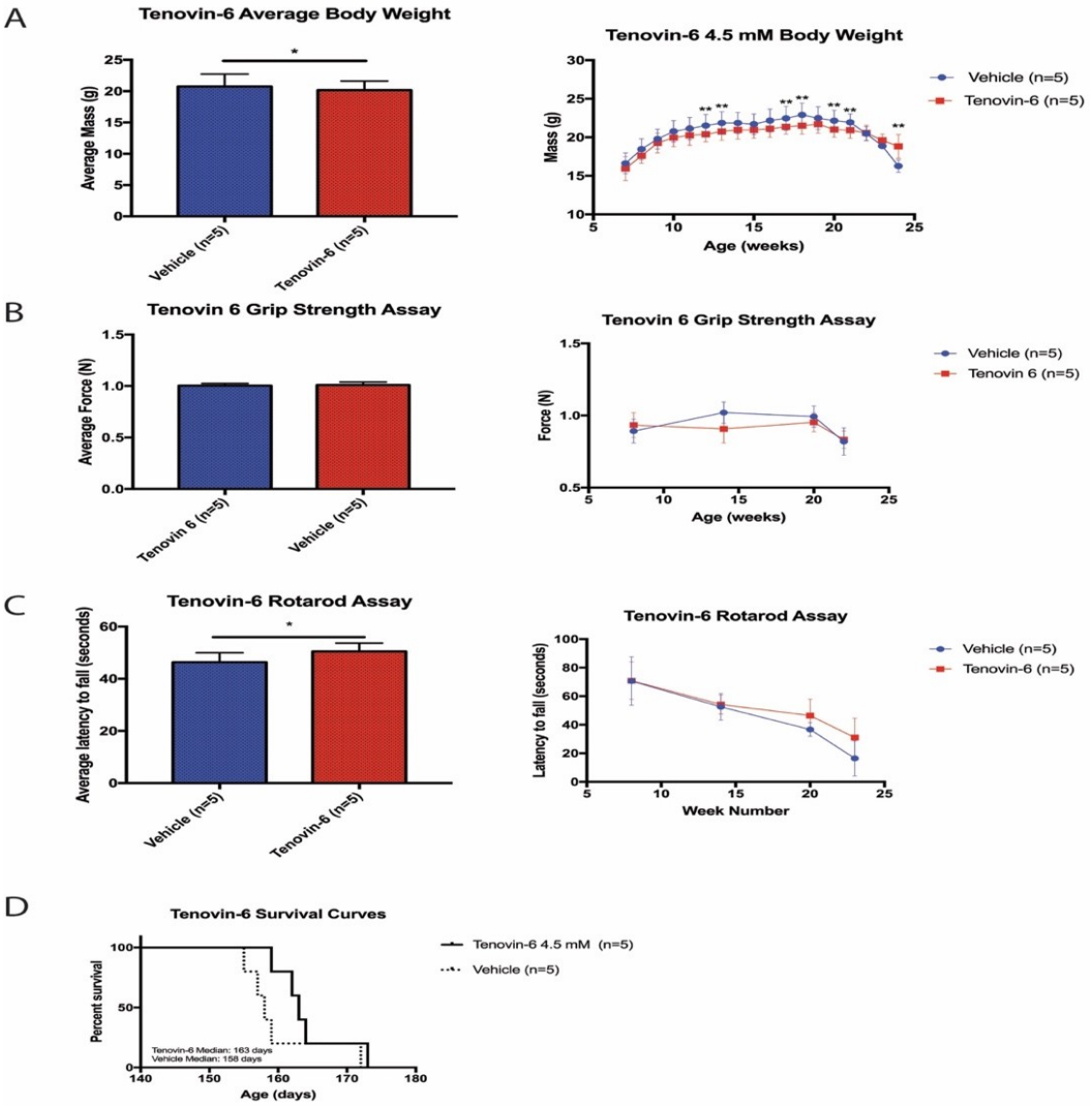

Fig. 5: (A) Tenovin-6 treated mice weighed less than vehicle controls but (B) performed the same as them on the grip strength assay. (C) Tenovin-6 treated mice had better locomotor activity during but (D) did no live significantly longer than the vehicle control.

Tenoving-6 4.5 mM did not significantly increase the lifespan of mice

Although the median life span of Tenovin-6 4.5 mM treated mice is 5 days more than that of the vehicle group and most Tenovin-6 4.5 mM treated mice met the euthanasia criteria after the vehicle, the difference is not significant (Fig. 6D). Both groups showed a similar trend.

Tenovin-6 4.5 mM did not delay the age of disease onset

The median age of onset for both groups was found to be similar. Upon reaching stage 5, mice on both groups lived for an average of two days before meeting the euthanasia criteria.

Discussion

Protein quality control is essential to ensure cellular homeostasis. Dysregulation of this process results in several pathological conditions including ALS which leads to a loss of motor neurons. While several genes play a role in disease development in concert, the focus of this project was to understand the therapeutic potential of small molecules that assist in degrading SOD1 aggregates by upregulating p53 mediated transcription. The common mouse model C57BL/6J containing the *SOD1*^{G93A} transgene was employed for this study. The mouse contains at least 23 copies of the transgene inserted into the genome, and maintaining the high copy number is essential for disease development(Scott et al., 2008) . Reports of copy number loss through homologous recombination resulting in a much later onset of disease have been published(Acevedo-Arozena et al., 2011; Alexander et al., 2004; Deitch et al., 2014; Scott et al., 2008) . However, the study design ensured that gender and litter-matched mice with high copy numbers were selected for experimentation.

p53 has been shown to be drastically elevated in brain and spinal cord tissue from mice and humans suffering from ALS, generating a long-standing hypothesis that immense upregulation results in motor neuron apoptosis(Barbosa et al., 2010; Eve, Dennis, & Citron, 2007; Martin, 2000) . However, a few studies challenged this notion and showed that p53 upregulation assists with protein quality control in ALS and Alzheimer's Disease models(Merlo et al., 2014; Periz et al., 2015), and that disease development is imminent regardless of p53 status(Prudlo et al., 2000) . UNC669 and Tenovin-6, both upregulate p53 mediated transcription in independent ways. UNC669 promotes recruitment of p53 to its promoter via SETD8 by inhibiting the histone-L3MBTL1 interaction(Arrowsmith et al., 2007; Klara Acs et al., 2011; Trojer et al., 2007) , while Tenovin-6 promotes p53

upregulation by inhibiting the protein deacetylases SIRT1/2(James T. Lee & Wei Gu, 2013; van Leeuwen et al., 2011) .

This study shows that p53 upregulation benefited neuromuscular activity in mice, which is analogous to improving quality of life in humans, but did not delay disease onset or increase life span. In addition, UNC669 (Fig. 2F, Fig. 2G) and Tenovin-6 reduced the number of large SOD1 aggregates (unpublished data, Goran Periz).

UNC669 showed a dose and age dependent response in mice (Fig. 2A, Fig. 2B, Fig. 2D, Fig. 2E, Fig. 2F, Fig. 3A, Fig. 3B, Fig. 3C). It is interesting to note that mice subjected to a 10 mM solution benefited from treatment, while those subjected to a 30 mM solution did not. This suggests a possible threshold of p53 activation to observe beneficial physiological effects, beyond which the apoptotic machinery is overworked and resulting in cell death. While this hypothesis was not examined by the study, immunohistochemical analyses of p53 from central nervous system tissue along with co-localization studies may provide insights to this interesting phenomenon. Furthermore, mice between the age group of 11-17 weeks (Fig. 2C) seemed to benefit from treatment the most. While the study examined bioavalability of UNC669 to the brain and spinal cord (Fig. 1C), one cannot rule out altered bioavailability at different age groups. Mice with ages varying from 6 weeks – 12 weeks were selected for mass spectrometry, and it is possible that bioavalability to the central nervous system may reduce with age. Furthermore, non-transgenic mice were selected for mass spectrometry and it has not been confirmed that the distribution of UNC669 in a non-transgenic mouse resembles that of $SOD1^{G93A}$ transgenic model.

Aggregation is a hallmark of SOD1-ALS. Large aggregates are extremely proteotoxic and provide greater surface are to sequester other proteins such as the anti-apoptotic Bcl-

2(Pasinelli et al., 2004) . UNC669 cleared large SOD1 aggregates but not smaller ones *in vitro* and *in vivo* (Fig. 2F, Fig. 2G) suggesting that a misfolding stress response was coming into play. Unperturbed levels of smaller aggregates and soluble $SOD1^{G93A/G85R}$ suggest that the effect may not be caused due to decreased transcription of $SOD1^{G93A/G85R}$ but increased protein degradation. Indeed, this was confirmed in a cycloheximide chase which showed greater degradation on knocking down L3MBTL1 as compared to the control (unpublished data, Goran Periz).

Tenovin-6 has been extensively studied for its role in protein quality control in models of neurodegenerative disease and cancer(Brooks & Gu, 2009; Hirai et al., 2014; Lane, Fersht, Brown, Verma, & Lain, 2009) . Upon questioning its distribution over time after an intraperitoneal injection, the study showed saturation kinetics in the brain and spinal cord. However, the concentration of Tenovin-6 in spinal cord samples at the 1.5 hour time point was significantly lower than that of the 0.5 hour and 3 hour time point (Fig. 4C). This is perplexing and may be dependent on the distribution of Tenovin-6 in cerebrospinal fluid and cells in the central nervous system.

The study showed that Tenovin-6 treated mice had better locomotor activity but lower body weight as compared to its control (Fig. 5A, Fig. 5C). This is perplexing as decreased body weight may be associated with a greater intensity of disease, while increased neuromuscular activity suggests protection from disease. Interestingly, Tenovin-6 benefited mice the most in the latter stages, suggesting that it is indeed protecting from disease. Furthermore, mice treated with Tenovin-6 weighed more than the control group at the time of euthanasia. These facts taken together suggest neuroprotective effects of Tenovin-6.

Lastly, these findings suggest that upregulating p53 may be a viable option to treat SOD1-ALS. Although it does not appear to delay disease onset or prolong lifespan, it has prominent effects on aggregation and neuromuscular activity. Since UNC669 and Tenovin-6 appear to have an age-dependent response in mice, using them in conjunction may be fruitful. Indeed, this study has not examined their exact mechanisms of action and future studies to elucidate their pathways will greatly benefit their therapeutic potential.

References

Acevedo-Arozena, A., Kalmar, B., Essa, S., Ricketts, T., Joyce, P., Kent, R., . . . Fisher, E. M. C. (2011). A comprehensive assessment of the SOD1G93A low-copy transgenic mouse, which models human amyotrophic lateral sclerosis. *Disease Models & Mechanisms, 4*(5), 686. doi:10.1242/dmm.007237

Alexander, G. M., Erwin, K. L., Byers, N., Deitch, J. S., Augelli, B. J., Blankenhorn, E. P., & Heiman-Patterson, T. D. (2004). Effect of transgene copy number on survival in the G93A SOD1 transgenic mouse model of ALS. *Molecular Brain Research, 130*(1), 7-15. doi:10.1016/j.molbrainres.2004.07.002

Arrowsmith, C. H., Nady, N., Allali-Hassani, A., Liu, Y., Qi, C., MacKenzie, F., . . . Ouyang, H. (2007). L3MBTL1 recognition of mono- and dimethylated histones. *Nature Structural & Molecular Biology, 14*(12), 1229-1230. doi:10.1038/nsmb1340

Barbosa, L. F., Cerqueira, F. M., Macedo, A. F. A., Garcia, C. C. M., Angeli, J. P. F., Schumacher, R. I., . . . Medeiros, M. H. G. (2010). Increased SOD1 association with chromatin, DNA damage, p53 activation, and apoptosis in a cellular model of SOD1-linked ALS. *Biochimica Et Biophysica Acta (BBA) - Molecular Basis of Disease, 1802*(5), 462-471. doi:10.1016/j.bbadis.2010.01.011

Brooks, C. L., & Gu, W. (2009). *Perspectives*. London: s.n. Retrieved from http://www.nature.com.ezp.welch.jhmi.edu.proxy1.library.jhu.edu/nrc/journal/v9/n2/full/nrc2562.html

Bruijn, L. I., Houseweart, M. K., Kato, S., Anderson, K. L., Anderson, S. D., Ohama, E., . . . Cleveland, D. W. (1998). Aggregation and motor neuron toxicity of an ALS-

linked SOD1 mutant independent from wild-type SOD1. *Science, 281*(5384), 1851-1854. Retrieved from http://www.jstor.org/stable/2895798

Bruijn, L. I., Miller, T. M., & Cleveland, D. W. (2004). Unraveling the mechanisms involved in motor neuron degradation in ALS. *Http://Dx.Doi.Org.Ezp.Welch.Jhmi.Edu/10.1146/Annurev.Neuro.27.070203.144244, 27*, 723-749. doi:10.1146/annurev.neuro.27.070203.144244

Bryson, H. M., & Bryson, H. M. (1996). A review of its pharmacodynamic and pharmacokinetic properties and therapeutic potential in amyotrophic lateral sclerosis. *Drugs, 52*(4), 549-563.

Corcia, P., Couratier, P., Blasco, H., Andres, C. R., Beltran, S., Meininger, V., & Vourc'h, P. (2017). Genetics of amyotrophic lateral sclerosis. *Revue Neurologique, 173*(5), 254-262. doi:10.1016/j.neurol.2017.03.030

Deitch, J. S., Alexander, G. M., Bensinger, A., Yang, S., Jiang, J. T., & Heiman-Patterson, T. D. (2014). Phenotype of transgenic mice carrying a very low copy number of the mutant human G93A superoxide dismutase-1 gene associated with amyotrophic lateral sclerosis. *PLoS ONE, 9*(6), 1-6. doi:10.1371/journal.pone.0099879

Eve, D. J., Dennis, J. S., & Citron, B. A. (2007). Transcription factor p53 in degenerating spinal cords. *Brain Research, 1150*, 174-181. doi:10.1016/j.brainres.2007.02.088

Hatzipetros, T., Kidd, J. D., Moreno, A. J., Thompson, K., Gill, A., & Vieira, F. G. (2015). A quick phenotypic neurological scoring system for evaluating disease progression in the SOD1-G93A mouse model of ALS. *Journal of Visualized Experiments: JoVE,* (104) doi:10.3791/53257

Herold, J. M., James, L. I., Korboukh, V. K., Gao, C., Coil, K. E., Bua, D. J., . . . Frye, S. V. (2012). Structure–activity relationships of methyl-lysine reader antagonists. *Med. Chem. Commun, 3*(1), 45-51. doi:10.1039/C1MD00195G

Hirai, S., Endo, S., Saito, R., Hirose, M., Ueno, T., Suzuki, H., . . . Hyodo, I. (2014). Antitumor effects of a sirtuin inhibitor, tenovin-6, against gastric cancer cells via death receptor 5 up-regulation. *PLoS ONE, 9*(7), 1-10. doi:10.1371/journal.pone.0102831

James T. Lee, & Wei Gu. (2013). *SIRT1: Regulator of p53 deacetylation reprints and permission:* SAGE Publications. doi:10.1177/1947601913484496

Jiang, H. -., Ren, M., Jiang, H. -., Wang, J., Zhang, J., Yin, X., . . . Feng, H. -. (2014). Guanabenz delays the onset of disease symptoms, extends lifespan, improves motor performance and attenuates motor neuron loss in the SOD1 G93A mouse model of amyotrophic lateral sclerosis. *Neuroscience, 277*, 132-138. doi:10.1016/j.neuroscience.2014.03.047

Kiernan, M. C., Vucic, S., Cheah, B. C., Turner, M. R., Eisen, A., Hardiman, O., . . . Zoing, M. C. (2011). Amyotrophic lateral sclerosis. *The Lancet, 377*(9769), 942-955. doi:10.1016/S0140-6736(10)61156-7

Kiernan, M. C., Vucic, S., Cheah, B. C., Turner, M. R., Eisen, A., Hardiman, O., . . . Zoing, M. C. (2011). Amyotrophic lateral sclerosis. *The Lancet, 377*(9769), 942-955. doi:10.1016/S0140-6736(10)61156-7

Klara Acs, Martijn S Luijsterburg, Leena Ackermann, Florian A Salomons, Thorsten Hoppe, & Nico P Dantuma. (2011). The AAA-ATPase VCP/p97 promotes 53BP1

recruitment by removing L3MBTL1 from DNA double-strand breaks. *Nature Structural & Molecular Biology, 18*(12), 1345-1350. doi:10.1038/nsmb.2188

Knippenberg, S., Thau, N., Dengler, R., & Petri, S. (2010). Significance of behavioural tests in a transgenic mouse model of amyotrophic lateral sclerosis (ALS). *Behavioural Brain Research, 213*(1), 82-87. doi:10.1016/j.bbr.2010.04.042

Lacomblez, L. (1996). Dose-ranging study of riluzole in amyotrophic lateral sclerosis. *Lancet, 347*(9013), 1425-1431.

Lane, D. P., Fersht, A. R., Brown, C. J., Verma, C. S., & Lain, S. (2009). Awakening guardian angels: Drugging the p53 pathway. *Nature Reviews Cancer, 9*(12), 862-873. doi:10.1038/nrc2763

Mancuso, R., Oliván, S., Rando, A., Casas, C., Osta, R., & Navarro, X. (2012). Sigma-1R agonist improves motor function and motoneuron survival in ALS mice. *Neurotherapeutics: The Journal of the American Society for Experimental NeuroTherapeutics, 9*(4), 814-826. doi:10.1007/s13311-012-0140-y

Mancuso, R., Valle, J. d., Modol, L., Martinez, A., Granado-Serrano, A. B., Ramirez-Núñez, O., . . . Navarro, X. (2014). Resveratrol improves motoneuron function and extends survival in SOD1G93A ALS mice. *Neurotherapeutics, 11*(2), 419. doi:10.1007/s13311-013-0253-y

Martin, L. J. (2000). p53 is abnormally elevated and active in the CNS of patients with amyotrophic lateral sclerosis. *Neurobiology of Disease, 7*(6), 613-622. doi:10.1006/nbdi.2000.0314

Merlo, P., Frost, B., Peng, S., Yang, Y. J., Park, P. J., & Feany, M. (2014). P53 prevents neurodegeneration by regulating synaptic genes. *Proceedings of the National*

Academy of Sciences of the United States of America, 111(50), 18055. doi:10.1073/pnas.1419083111

Pasinelli, P., Belford, M. E., Lennon, N., Bacskai, B. J., Hyman, B. T., Trotti, D., & Brown, R. H. (2004). Amyotrophic lateral sclerosis-associated SOD1 mutant proteins bind and aggregate with bcl-2 in spinal cord mitochondria. *Neuron, 43*(1), 19-30. doi:10.1016/j.neuron.2004.06.021

Periz, G., Lu, J., Zhang, T., Kankel, M. W., Jablonski, A. M., Kalb, R., . . . Wang, J. (2015). Regulation of protein quality control by UBE4B and LSD1 through p53-mediated transcription. *PLoS Biology, 13*(4) doi:10.1371/journal.pbio.1002114

Prathyusha Vikram, P., Shanmugasundaram. (2017). Determination of riluzole in human plasma by ultra performance liquid chromatography - tandem mass spectrometry (UPLC - MS/MS) and its application to a pharmacokinetic study.*10*(1), 193-199. Retrieved from https://search-proquest-com.ezp.welch.jhmi.edu/docview/1875652183?accountid=11752

Prudlo, J., Koenig, J., Gräser, J., Burckhardt, E., Mestres, P., Menger, M., & Roemer, K. (2000). Motor neuron cell death in a mouse model of FALS is not mediated by the p53 cell survival regulator. *Brain Research, 879*(1), 183-187. doi:10.1016/S0006-8993(00)02745-1

Rachele A Saccon, Rosie K A Bunton-Stasyshyn, Elizabeth M C Fisher, & Pietro Fratta. (2013). *Is SOD1 loss of function involved in amyotrophic lateral sclerosis?*. England: doi:10.1093/brain/awt097

Rosen, D. R., Siddique, T., Patterson, D., Figlewicz, D. A., Sapp, P., Hentati, A., . . . Brown, R. H. (1993). *Mutations in cu/zn superoxide dismutase gene are associated*

with familial amyotrophic lateral sclerosis Nature Publishing Group. doi:10.1038/362059a0

Scott, S., Kranz, J. E., Cole, J., Lincecum, J. M., Thompson, K., Kelly, N., . . . Heywood, J. A. (2008). Design, power, and interpretation of studies in the standard murine model of ALS. *Amyotrophic Lateral Sclerosis, 9*(1), 4-15. doi:10.1080/17482960701856300

Smittkamp, S. E., Brown, J. W., & Stanford, J. A. (2008). Time-course and characterization of orolingual motor deficits in B6SJL-tg(SOD1-G93A)1Gur/J mice. *Neuroscience, 151*(2), 613-621. doi:10.1016/j.neuroscience.2007.10.017

Talbott, E. O., Malek, A. M., & Lacomis, D. (2016). *The epidemiology of amyotrophic lateral sclerosis* doi:10.1016/B978-0-12-802973-2.00013-6

Traynor, B. J., Bruijn, L., Conwit, R., Beal, F., O'Neill, G., Fagan, S. C., & Cudkowicz, M. E. (2006). Neuroprotective agents for clinical trials in ALS A systematic assessment. *Neurology, 67*(1), 20-27. doi:10.1212/01.wnl.0000223353.34006.54

Trojer, P., Li, G., Sims, R. J., Vaquero, A., Kalakonda, N., Boccuni, P., . . . Reinberg, D. (2007). L3MBTL1, a histone-methylation-dependent chromatin lock. *Cell, 129*(5), 915-928. doi:10.1016/j.cell.2007.03.048

van Leeuwen, I. M. M., Higgins, M., Campbell, J., Brown, C. J., McCarthy, A. R., Pirrie, L., . . . Laín, S. (2011). Mechanism-specific signatures for small-molecule p53 activators. *Cell Cycle, 10*(10), 1590-1598. doi:10.4161/cc.10.10.15519

Watanabe, M., Dykes-Hoberg, M., Cizewski Culotta, V., Price, D. L., Wong, P. C., & Rothstein, J. D. (2001). Histological evidence of protein aggregation in mutant SOD1

transgenic mice and in amyotrophic lateral sclerosis neural tissues. *Neurobiology of Disease, 8*(6), 933-941. doi:10.1006/nbdi.2001.0443

Wilson, J. M. B., Petrik, M. S., Moghadasian, M. H., & Shaw, C. A. (2005). Examining the interaction of apo E and neurotoxicity on a murine model of ALS-PDC. *Canadian Journal of Physiology and Pharmacology, 83*(2), 131-141. doi:10.1139/y04-140

Yasuda, K., Clatterbuck-Soper, S. F., Jackrel, M. E., Shorter, J., & Mili, S. (2017). FUS inclusions disrupt RNA localization by sequestering kinesin-1 and inhibiting microtubule detyrosination. *The Journal of Cell Biology, 216*(4), 1015-1034. doi:10.1083/jcb.201608022

Zhou, H., Che, X., Bao, G., Wang, N., Peng, L., Barnash, K. D., . . . Bai, X. (2016). Design, synthesis, and protein methyltransferase activity of a unique set of constrained amine containing compounds. *Bioorganic & Medicinal Chemistry Letters, 26*(18), 4436-4440. doi:10.1016/j.bmcl.2016.08.004

YAJAS SHAH

325 East University Parkway
Baltimore, MD 21218
(M) +1 470-985-4711 | yshah2@jhmi.edu

EDUCATION

Master of Science (ScM) Expected August 2017
Johns Hopkins Bloomberg School of Public Health, Baltimore, MD
Concentration: Biochemistry and Molecular Biology
Relevant Coursework: Genomics for Public Health, Molecular Toxicology, Cellular Stress in Physiology and Disease, Genome Integrity and Cancer, Immunology Infection and Disease, Statistical Reasoning in Public Health I, Practical Epidemiology for Basic Scientists

Bachelor of Science (BSc) April 2014
University of Mumbai, India
Majors: Biochemistry and Life Sciences

EXPERIENCE

Graduate Student Aug. 2015 – Present
Johns Hopkins Bloomberg School of Public Health, Baltimore, MD

- Collected, organized, and compiled data pertaining to a project that studies the effect of candidate drugs in preclinical trials conducted in murine models of ALS
- Conducted extensive *in vitro* and *in vivo* studies including drug dosage (IP) and tissue harvest for pharmacokinetic studies
- Evaluated the efficacy of candidate drugs through biochemical and behavioral assays in rodent models of ALS as well as mammalian cell lines
- Optimized PCR genotyping protocols, and gained extensive knowledge of mouse genetics, mouse handling, surgery, necropsy, dissection and breeding
- Assisted with iPSC culture

Clinical Research Assistant Mar. – Jul. 2015
Department of Clinical Research, National Institute for Research in Reproductive Health, Mumbai, India

- Established and standardized PCR protocols
- Conducted genotyping experiments and analyzed genome sequencing data to identify novel polymorphisms in the *CFTR* gene
- Assisted with genetic counselling of patients suffering from Congenital Bilateral Absence of the Vas Deferens (CBAVD)

Research Assistant May – July 2013
Department of Biochemistry, National Institute for Research in Reproductive Health, Mumbai, India

- Performed biochemical assays to detect the prevalence of HIV in clinical samples
- Collected, compiled and cataloged the data obtained

Intern Jan. – June 2011

Samit Diagnostic Centre, Mumbai, India

- Assisted a diagnostic laboratory with techniques ranging from PCR, ELISA, agarose gel electrophoresis and other biochemical tests

Intern June – Dec. 2010

Eyeglobal Technologies Pvt. Ltd., Mumbai, India

- Assisted in business development, customer relationship management, staffing and other operational functions of the human resource management company

Intern Nov. 2009 – May 2010

Ronuplate Pvt. Ltd., Mumbai, India

- Assisted with quality control in an electroplating plant

PUBLICATIONS AND CONFERENCES

- Langseth, J.A., Kim, J., Ugolino, J., **Shah, Y.**, Hwang, H., Wang, J., Bergles, D., Brown, S. (2017). Cell-type specific differences in promoter activity of the ALS-linked C9orf72 mouse ortholog. *Scientific Reports*.
- Presented research "*New Players in Protein Quality Contro*l" at the Department of Biochemistry and Molecular Biology Retreat (April, 2017)
- **Shah, Y.**, Rai, S. and Vajpai, A. (2014). Current advances in the use of phytochemicals for the treatment of Obesity: A Review. *Jigyasa*, 10(1), pp.63-69.
- Individually presented paper entitled "*Current advances in the use of phytochemicals for the treatment of Obesity: A Review*" at the University Grants Commission Research Scholars' Meet (January, 2014)

HONORS AND AWARDS

- Science Honors (2014)

PROFESSIONAL DEVELOPMENT

- Mentorship: Mentoring two Masters students (April, 2017 – current)
- Computer Skills: Microsoft Office Suite, Adobe Illustrator, Adobe Photoshop, Adobe Indesign, Graphpad Prism, ImageJ
- Laboratory Techniques:
    - Molecular Biology: DNA/RNA isolation, PCR, qPCR, SDS-PAGE, Agarose Gel Electrophoresis, Western Blot, ELISA (for p24), , Molecular cloning, Protein extraction, Protein fractionation
    - Cell Biology: Mammalian cell culture (HEK293T, HeLa, MEF, Vk2/E6E), iPSC culture, PBMC isolation, Fluorescence microscopy
    - Animal Models: Surgery, Dissection, Tissue harvest, Necropsy, Transcardial perfusion, Drug dosing (IP), Mouse genetics, Animal handling, Mouse breeding, Retro-orbital sinus bleeding, Genotyping, Behavioral assays
    - Spectroscopy: UV-Vis Spectroscopy

- Memberships and Leadership Positions:
    - 2016: American Society for Biochemistry and Molecular Biology, JHSPH Student Assembly
    - 2015: JHSPH Sustainability Liaison, JHU Indian Graduate Students Association
    - 2011: KC College Public Relations Team